

DTP-97-67  
KCL-MTH-97-71  
SPhT-97/163  
hep-th/9712197  
December 1997  
(revised)

## TBA and TCSA with boundaries and excited states

Patrick Dorey<sup>1</sup>, Andrew Pocklington<sup>1</sup>, Roberto Tateo<sup>2</sup> and Gérard Watts<sup>3</sup>

<sup>1</sup>*Department of Mathematical Sciences,  
University of Durham, Durham DH1 3LE, England*

<sup>2</sup>*Service de Physique Théorique, CEA-Saclay,  
F-91191 Gif-sur-Yvette Cedex, France*

<sup>3</sup>*Mathematics Department,  
King's College London, Strand, London WC2R 2LS, U.K.*

### Abstract

We study the spectrum of the scaling Lee-Yang model on a finite interval from two points of view: via a generalisation of the truncated conformal space approach to systems with boundaries, and via the boundary thermodynamic Bethe ansatz. This allows reflection factors to be matched with specific boundary conditions, and leads us to propose a new (and non-minimal) family of reflection factors to describe the one relevant boundary perturbation in the model. The equations proposed previously for the ground state on an interval must be revised in certain regimes, and we find the necessary modifications by analytic continuation. We also propose new equations to describe excited states, and check all equations against boundary truncated conformal space data. Access to the finite-size spectrum enables us to observe boundary flows when the bulk remains massless, and the formation of boundary bound states when the bulk is massive.

---

<sup>1</sup>e-mail: P.E.Dorey@durham.ac.uk, A.J.Pocklington@durham.ac.uk

<sup>2</sup>e-mail: Tateo@wasa.saclay.cea.fr

<sup>3</sup>e-mail: gmtw@mth.kcl.ac.uk

# 1 Introduction

Integrable quantum field theories in domains with boundaries have attracted some attention of late, principally in the wake of a paper by Ghoshal and Zamolodchikov [1]. Such theories can be specified in terms of ultraviolet data consisting of the original boundary conformal field theory together with a specification of the particular perturbations chosen, both in the bulk and/or at the boundary, or else in terms of infrared data, which might consist of a bulk S-matrix together with a set of reflection factors encoding the scattering of each particle in the model off a single boundary. The reflection factors are constrained by various consistency conditions – unitarity, crossing-unitarity [1], and the boundary Yang-Baxter [2] and boundary bootstrap [1,3] equations – and it is natural to explore the space of solutions to these conditions, and then attempt to match them with particular perturbed boundary conformal field theories. While the first aspect has been studied by many authors, the second is comparatively underdeveloped, and provides much of the motivation for the work to be described in this paper. The strategy (already employed with much success in boundaryless situations) will be to study finite-volume spectra by two different routes, one based on the ultraviolet data and one on the infrared data, and then to compare the results. The ultraviolet route will proceed via a generalisation of the truncated conformal space approach (TCSA) [4] to boundary situations. This seems to us to be of independent interest, and should be useful in non-integrable situations too. For brevity, we shall refer to this method as the BTCSA, for boundary truncated conformal space approach. On the infrared side, the main weapon will be the ‘BTBA’, a modification of the thermodynamic Bethe ansatz (TBA) equations [5] adapted to boundary situations, introduced in refs. [6,7]. We have made a study of the analytic structure of these modified equations, uncovering a number of surprises along the way. We have also found new equations, some of them encoding the ground state energy in regimes where the previously-proposed equations break down, and others the energies of excited states. These new equations are similar in form to those found in [8,9] for excited states in the more traditional (boundaryless) TBA. The agreement between BTCSA and BTBA results offers support for both, and in addition allows us to obtain concrete predictions about the relationship between various parameters appearing at short and long distances.

Thus far, most of our work has been confined to what appears to be the simplest nontrivial example, namely the boundary scaling Lee-Yang model, but the methods advocated certainly have wider applicability. In this paper the emphasis will be on the structure of the BTBA equations and the matching of their solutions with the results that we have obtained by means of the BTCSA. A more detailed description of the BTCSA method itself will appear in a companion paper, currently in preparation [10].

## 2 The model

The ultraviolet limit of the scaling Lee-Yang model (SLYM) is the  $\mathcal{M}(2/5)$  minimal model [11], a non-unitary conformal field theory with central charge  $c = -22/5$ . The field content and the operator description depends on the geometry considered, but far from any boundary the local fields are those of the theory on a plane, and are left and right Virasoro descendants of the primary fields  $\mathbb{1}$ , of scaling dimension 0, and  $\varphi$ , of scaling dimension  $x_\varphi = \Delta_\varphi + \bar{\Delta}_\varphi = -2/5$ . Both of these are scalars, and the one non-trivial fusion rule is  $\varphi \times \varphi = \mathbb{1} + \varphi$ . The conventional normalisation of  $\varphi$  is

$$\varphi(z) \varphi(w) = |z - w|^{4/5} + C_{\varphi\varphi}^\varphi \varphi(w) |z - w|^{2/5} + \dots, \quad (2.1)$$

but this results in  $C$  being purely imaginary, and many other structure constants in the boundary theory being imaginary as well. For this reason, we have chosen the non-standard normalisation

$$\varphi(z) \varphi(w) = -|z - w|^{4/5} + C_{\varphi\varphi}^\varphi \varphi(w) |z - w|^{2/5} + \dots, \quad (2.2)$$

where we take  $C_{\varphi\varphi}^\varphi = -C_{\varphi\varphi}^\varphi$  to be a positive real number.

If the physical geometry has a boundary, then a conformally invariant boundary condition (CBC) must be assigned to each component of that boundary, and the possible local fields on any part of the boundary depend on the particular conformal boundary condition found there. Cardy has classified the possible boundary conditions [12] and the field content on each of these can be found by solving the consistency conditions given by Cardy and Lewellen [13]. The boundary fields fall into irreducible representations of a single Virasoro algebra, so all that is needed to specify the local field content of a particular conformally invariant boundary condition is the set of weights of the primary boundary fields.

It turns out that there are two conformal boundary conditions for  $\mathcal{M}(2/5)$ , which by an abuse of notation we shall label by  $\mathbb{1}$  and  $\Phi$ . The  $\mathbb{1}$  boundary has only one primary boundary field, which is the identity  $\mathbb{1}$ , while the  $\Phi$  boundary has two, the identity and a field  $\phi$  of scaling dimension  $x_\phi = -1/5$ . As a result, there are no relevant boundary perturbations of the  $\mathbb{1}$  boundary, and a single relevant perturbation of the  $\Phi$  boundary, by the field  $\phi$ . As with equation (2.2), we choose the normalisation of  $\phi$  to be

$$\phi(x) \phi(y) = -|x - y|^{2/5} + C_{\phi\phi}^\phi \phi(y) |x - y|^{1/5} + \dots, \quad (2.3)$$

with  $C_{\phi\phi}^\phi = -C_{\phi\phi}^\phi$  a positive real number. Together equations (2.2) and (2.3) determine the bulk-boundary constant  ${}^\Phi B_\varphi^\phi$  appearing in the expansion of  $\varphi(x + iy)$  on the upper half plane with boundary condition  $\Phi$  at  $y = 0$ :

$$\varphi(x + iy) = {}^\Phi B_\varphi^\phi \phi(x) (2y)^{1/5} + \dots. \quad (2.4)$$

The only remaining independent structure constant appears in the operator product expansion of two boundary-changing operators, but is not needed to reproduce the results in this paper.

This sketch will suffice for a description of the various boundary scaling Lee-Yang models that we shall be considering. Each can be regarded as a perturbation of one of the boundary conformal field theories just discussed.

First, suppose that there is no boundary at all. There is only the bulk to perturb, and if the perturbation is to be relevant then there is only one bulk field, namely  $\varphi$ , to perturb by. The perturbed action

$$\mathcal{A}_{\text{SLYM}} = \mathcal{A}_{\mathcal{M}(2/5)} + \lambda \int_{-\infty}^{\infty} dy \int_{-\infty}^{\infty} dx \varphi(x, y) \quad (2.5)$$

is integrable, and, for  $\lambda > 0$ , results in a massive scattering theory with a single particle type of mass  $M$ , and two-particle S-matrix [14]

$$S(\theta) = - (1) (2) \quad , \quad (x) = \frac{\sinh(\frac{\theta}{2} + \frac{i\pi x}{6})}{\sinh(\frac{\theta}{2} - \frac{i\pi x}{6})} . \quad (2.6)$$

The exact relationship between  $M$  and  $\lambda$  was found in [15]. In the conventions implied by (2.2) and (2.5), it is

$$M(\lambda) = \frac{2^{19/12} \sqrt{\pi} (\Gamma(3/5)\Gamma(4/5))^{5/12}}{5^{5/16} \Gamma(2/3)\Gamma(5/6)} \lambda^{5/12} = (2.642944 \dots) \lambda^{5/12} . \quad (2.7)$$

Now add a single boundary along the imaginary axis  $x = 0$ . Then, as explained in, for example, [1], the S-matrix should be supplemented with a reflection factor encoding how the particle bounces off the boundary. There are four ‘minimal’ possibilities, each of which satisfies all of the consistency conditions entailed by the S-matrix while minimising the number of poles and zeroes in the strip  $0 \leq \text{Im } \theta \leq \pi^*$ :

$$\begin{aligned} R_{(1)} &= \left(\frac{1}{2}\right) \left(\frac{3}{2}\right) \left(\frac{4}{2}\right)^{-1} \quad , \quad R_{(2)} = \left(\frac{3}{2}\right)^{-1} \left(\frac{4}{2}\right)^{-1} \left(\frac{5}{2}\right)^{-1} \\ R_{(3)} &= -\left(\frac{1}{2}\right) \left(\frac{2}{2}\right) \left(\frac{3}{2}\right) \quad , \quad R_{(4)} = -\left(\frac{2}{2}\right) \left(\frac{3}{2}\right)^{-1} \left(\frac{5}{2}\right)^{-1} \end{aligned} \quad (2.8)$$

The first two were given in [1], while the second two are related to these by multiplication by the bulk S-matrix. (As observed in [16], this procedure automatically generates further solutions to the consistency conditions.) In fact, an easing of the minimality requirement will be required in order to match all of the boundary conditions that will be encountered. For the time being we just note that the reflection factor

$$R_b(\theta) = \left(\frac{1}{2}\right) \left(\frac{3}{2}\right) \left(\frac{4}{2}\right)^{-1} \left(\frac{1-b}{2}\right)^{-1} \left(\frac{1+b}{2}\right) \left(\frac{5-b}{2}\right) \left(\frac{5+b}{2}\right)^{-1} \quad (2.9)$$

---

\*It might be more natural to minimise the number of poles and zeroes in the narrower strip  $0 \leq \text{Im } \theta \leq \pi/2$ . In any event, we won't be imposing either version of minimality, but rather checking solutions directly against BTCSA data.

is consistent with the bulk S-matrix for any value of the parameter  $b$ , and reduces to  $R_{(1)}$ ,  $R_{(2)}$  and  $R_{(3)}$  for  $b = 0$ ,  $-2$  and  $1$  respectively.

At this stage there is no way of telling which, if any, of these solutions is actually realised as the reflection factor of a concrete perturbed boundary conformal field theory. Such a theory, in the geometry currently under consideration, will have an action of the form

$$\mathcal{A}_{\text{BSLYM}} = \mathcal{A}_{\mathcal{M}(2/5)+\text{CBC}} + \lambda \int_{-\infty}^{\infty} dy \int_{-\infty}^0 dx \varphi(x, y) + h \int_{-\infty}^{\infty} dy \phi_B(y), \quad (2.10)$$

where  $\mathcal{A}_{\mathcal{M}(2/5)+\text{CBC}}$  is the action for the conformal field theory on the semi-infinite plane, with a definite conformal boundary condition at  $x = 0$ , and  $\phi_B(y)$  is one of the boundary fields allowed by that same boundary condition. We shall denote the boundary  $\Phi$  with a term in the action  $h \oint ds \phi(s)$  by  $\Phi(h)$ . It is important to appreciate that since the bulk-boundary coupling  $\Phi B_{\varphi}^{\phi}$  is non-zero, the sign of  $h$  is important, just as the fact that the bulk three-point coupling is non-zero means that the sign of  $\lambda$  in (2.5) and (2.10) is important.

As a final step, we add a second boundary to confine the system to a strip of finite width. The next section outlines how this situation can be analysed numerically, using a modification of the TCSA technique.

### 3 Boundary TCSA

The TCSA method of [4] assumes periodic boundary conditions, and has to be adapted to our context of a strip of width  $R$ . A conformal mapping from the strip to the upper half plane sends the quantisation surface to a semi-circle of radius 1, with the left and right boundary-perturbing operators sitting on the real axis at  $-1$  and  $1$  respectively. The Hamiltonian is then given in terms of the boundary conformal field theory as

$$H_{\alpha\beta}(M, R) = \frac{\pi}{R} \left[ L_0 - \frac{c}{24} + \lambda \left( \frac{R}{\pi} \right)^{2-x_{\varphi}} \int_0^{\pi} d\theta \varphi(\exp(i\theta)) \right. \\ \left. + h_L \left( \frac{R}{\pi} \right)^{1-x_L} \phi_L(-1) + h_R \left( \frac{R}{\pi} \right)^{1-x_R} \phi_R(1) \right], \quad (3.1)$$

where  $\varphi$  is the bulk primary field and  $\phi_L$  and  $\phi_R$  are the boundary perturbations (if any) applied to the left and right boundaries of the strip. The scaling dimensions of these operators are  $x_{\varphi}$ ,  $x_L$  and  $x_R$  respectively. The subscripts  $\alpha$  and  $\beta$  of  $H_{\alpha\beta}(M, R)$  are included as reminders of the information residing in the left and right boundary conditions and perturbations, while  $M$  is related to the bulk coupling  $\lambda$  according to the relation (2.7). Since we are dealing here with relevant perturbations of the

scaling Lee-Yang model,  $x_\phi$  is equal to  $-2/5$ , and each of  $\phi_L$  and  $\phi_R$  is either absent, or is the boundary field  $\phi$  with scaling dimension  $x_\phi = -1/5$ . This latter option only arises when perturbing  $\Phi$  boundaries – as mentioned in the last section, the  $\mathbb{1}$  boundary does not support any relevant boundary perturbations.

The essence of the BTCSA is to diagonalise the Hamiltonian (3.1) in a finite-dimensional subspace of the full Hilbert space, usually obtained by discarding those states of conformal weight larger than some cutoff. The matrix elements of the fields  $\phi_L(-1)$ ,  $\phi_R(1)$  and  $\varphi(\exp(i\theta))$  can be found exactly, but in general the integral over  $\theta$  in (3.1) has been performed numerically.

If the Hilbert space of the model on a strip with conformal boundary conditions  $\alpha$  and  $\beta$  is  $\mathcal{H}_{(\alpha,\beta)}$ , and the irreducible Virasoro representation of weight  $h$  is  $V_h$ , then using [12] we found

$$\mathcal{H}_{(\mathbb{1},\mathbb{1})} = V_0, \quad \mathcal{H}_{(\mathbb{1},\Phi)} = V_{-1/5}, \quad \mathcal{H}_{(\Phi,\Phi)} = V_0 \oplus V_{-1/5}. \quad (3.2)$$

The full set of structure constants and correlation functions necessary to evaluate (3.1) on these spaces can then be found using [13], and will be given in [10].

We used the BTCSA to investigate the model with a pure boundary perturbation ( $\lambda=0$ ), and also with combined bulk / boundary perturbations. In the first case, perturbing by a relevant boundary field while leaving the bulk massless gives a renormalisation group flow which, while leaving the bulk properties of the conformal field theory unchanged, moves from one conformal boundary condition to another. The simplest context where we can study this phenomenon within the BTCSA is the bulk-conformal Lee-Yang model on a strip with  $(\mathbb{1}, \Phi)$  boundary conditions. Perturbing the  $\Phi$  boundary by the  $\phi$  field should provoke a flow to another conformal boundary condition with fewer relevant boundary operators. The only candidate is  $\mathbb{1}$ , and that is indeed what we found for *positive* values of  $h \equiv h_R$ . Since the bulk is massless, the only length scale in the problem is provided by the boundary field  $h$ , and the crossover occurs as a function of the dimensionless quantity  $r = h^{5/6}R$ . The best signal is provided by a plot of scaling functions, which we define in terms of the energy levels  $E_n(h, R)$  by

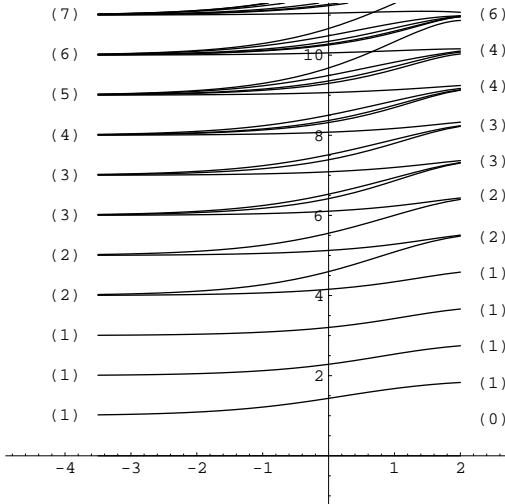
$$E_n(h, R) = \frac{\pi}{R} F_n(h^{5/6}R). \quad (3.3)$$

In figure 1a we display the gaps  $(F_n(r) - F_0(r))$  for the  $(\mathbb{1}, \Phi(h))$  boundary conditions with  $\log(r^{6/5}) = \log(hR^{6/5})$  varying from  $-4.9$  to  $2.7$ , using the BTCSA truncated to 98 states. We have used a logarithmic scale for to highlight the crossover region, in which there is a smooth flow between the  $\mathcal{H}_{(\mathbb{1},\Phi)}$  and  $\mathcal{H}_{(\mathbb{1},\mathbb{1})}$  spectra. As should be clear from the plot, the levels move from the degeneracy pattern given by  $\chi_{-1/5}$ , the

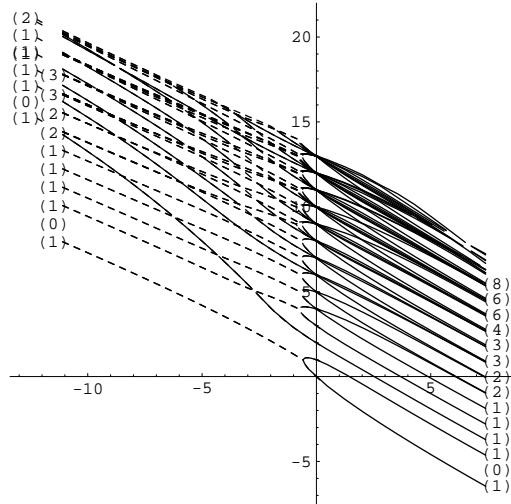
character of the  $V_{-1/5}$  representation, to that given by  $\chi_0$  :

$$\begin{aligned}
q^{1/60} \chi_{-1/5}(q) &= \\
&1 + q + q^2 + q^3 + 2q^4 + 2q^5 + 3q^6 + 3q^7 + 4q^8 + 5q^9 + 6q^{10} + 7q^{11} + O(q^{12}), \\
q^{-11/60} \chi_0(q) &= \\
&1 + q^2 + q^3 + q^4 + q^5 + 2q^6 + 2q^7 + 3q^8 + 3q^9 + 4q^{10} + 4q^{11} + O(q^{12}).
\end{aligned}
\tag{3.4}$$

With  $h$  *negative* the energies become complex at large (real)  $R$ , just as happens in the bulk if  $\lambda$  is negated [4]. However, in this case the spectrum remains identifiable. For large negative  $h$ , it splits into three components. There are two complex conjugate sets, the real parts of which are counted by the character  $\chi_0(q)$ ; and a third set which is real and which is also counted by the character  $\chi_0(q)$ , but which appears to have a different asymptotic behaviour in  $h$  and to decouple in the  $h \rightarrow \infty$  limit. To illustrate this point, in figure 1b we plot the first 53 scaling functions against  $r^{6/5} = hR^{6/5}$ , for  $-12.2 < hR^{5/6} < 7.4$ . The solid lines indicate real eigenvalues, and the dashed lines the real parts of complex eigenvalues. At the moment we are unsure quite what the interpretation of these complex eigenvalues is, or why the different components should be organised into representations of the Virasoro algebra. However similar spectra have been found before, for example see ref. [17].



1a) The excited state scaling function gaps as a function of  $\log(r^{6/5})$  for the  $M=0$  LY model on a strip with boundary conditions  $(\mathbb{1}, \Phi(h))$ , with  $h = (r/R)^{6/5}$ . The multiplicities are in parentheses.



1b) The first 53 scaling functions  $F_n(r)$  plotted against  $r^{6/5}$  for the  $M=0$  LY model on a strip with boundary conditions  $(\mathbb{1}, \Phi(h))$ , with  $h = (r/R)^{6/5}$ . The multiplicities are in parentheses.

We have also used the BTCSA to investigate massless boundary flows for other

unitary and non-unitary minimal models, with both integrable and non-integrable boundary perturbations. In unitary cases the spectrum remains real, but in other respects the picture just outlined seems to be rather general. More work will be needed before the full picture is clear, but one particular point is worth stressing: if the bulk is *massless*, then a boundary perturbation cannot affect this, and hence *any* boundary perturbation, integrable or non-integrable, must flow to a conformal, and indeed integrable, boundary condition under the renormalisation group. This contrasts with the generic behaviour of a bulk perturbation, where fine-tuning is required if the infrared limit is to be anything other than massive. It also helps to explain why we were able to observe massless boundary flows in the BTCSA, despite the errors caused by the truncation to a finite number of levels. In analogous bulk situations, the TCSA makes a rather bad job of modelling bulk-massless flows, even in situations where the oppositely-perturbed, bulk-massive, flows are captured fairly well – see for example section 5.2 of [18].

As a second application of the BTCSA, we have investigated combined bulk / boundary perturbations in order to unravel the connection between the reflection factors (2.8), (2.9) and particular perturbed boundary conformal field theories. To this end it is only necessary to consider the  $(\mathbb{1}, \mathbb{1})$  and  $(\mathbb{1}, \Phi(h))$  boundary conditions, but we defer the presentation of these results until later in the paper, after the discussion of the BTBA method.

Finally, we have used the BTCSA to investigate the complete partition function of the scaling Lee-Yang model on a cylinder of length  $R$  and circumference  $L$ , with bulk mass  $M$  and general boundary conditions  $(\alpha, \beta)$  at the two ends of the cylinder. In terms of the spectrum of the strip Hamiltonian (3.1), this partition function is

$$\begin{aligned} Z_{\alpha\beta}(M, R, L) &= \text{Tr}_{\mathcal{H}_{(\alpha,\beta)}} e^{-LH_{\alpha\beta}(M,R)} \\ &= \sum_{E_n \in \text{spec}(H_{\alpha\beta}(M,R))} \exp(-LE_n) . \end{aligned} \quad (3.5)$$

This partition function can also be evaluated by propagating states along the length of the cylinder, giving the large- $R$  asymptotic

$$Z_{\alpha\beta}(M, R, L) \sim_{R \rightarrow \infty} A_{\alpha\beta}(M, L) \exp(-R E_0^{\text{p}}(M, L)) \quad (3.6)$$

where  $E_0^{\text{p}}(M, L)$  is the ground state energy of the model on a circle of circumference  $L$ . The linear part of  $\log A_{\alpha\beta}$  can be extracted by setting

$$\log(A_{\alpha\beta}(M, L)) = \log(g_{\alpha}(M, L) g_{\beta}(M, L)) + B_{\alpha\beta} L , \quad (3.7)$$

For the two boundary conditions we have, the two functions  $g_{\mathbb{1}}(M, L)$  and  $g_{\Phi(h)}(M, L)$  can be expressed in terms of dimensionless combinations as

$$g_{\mathbb{1}}(M, L) = f_1(ML) , \quad g_{\Phi(h)}(M, L) = f_2(ML, hL^{6/5}) . \quad (3.8)$$



The numbers  $f_1(0)$  and  $f_2(0,0)$  are the “universal ground state degeneracies” discussed in [19] of the corresponding UV conformal boundary conditions, i.e.  $\mathbb{1}$  and  $\Phi(0)$  respectively, with values as given in table 1. The opposite,  $L \rightarrow \infty$ , limit must be taken with more care, as results are different for the two cases of massless and massive bulk.

At  $M=0$  (critical bulk), for  $h > 0$  the function  $f_2(0, hL^{6/5})$  governs the crossover between conformal boundary conditions  $\Phi(0)$  and  $\mathbb{1}$ , so that we expect [19]

$$\lim_{\substack{L \rightarrow \infty \\ h > 0}} g_{\Phi(h)}(0, L) = \lim_{\kappa \rightarrow +\infty} f_2(0, \kappa) = f_1(0) . \quad (3.9)$$

However, for a massive bulk, we expect that the limit  $L \rightarrow \infty$  will lead to a purely massive boundary theory, for which the ground state degeneracy is 1, so that in all cases for the Lee-Yang model,

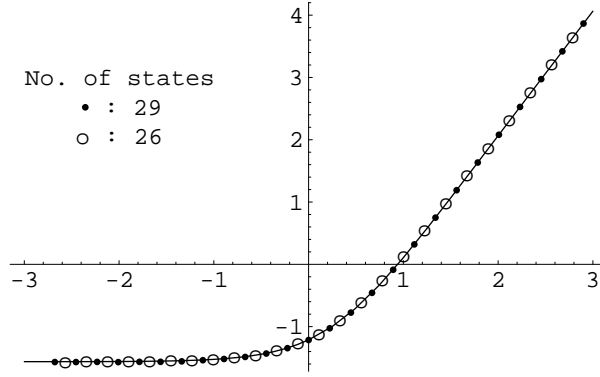
$$\lim_{\substack{L \rightarrow \infty \\ M > 0}} g_{\alpha}(M, L) = 1 . \quad (3.10)$$

The quantities that we have just been discussing arise in a limit where the formula (3.5) might be expected to break down, at least when truncated to a finite number of levels. Nevertheless, it turned out to be possible to extract both  $E_0^{\text{p}}(M, L)/M$  and the product  $g_{\alpha}(M, L)g_{\beta}(M, L)$  from the numerical approximation to the partition function as calculated from the spectrum of the BTCSA Hamiltonian.

As a first example, we calculated  $\log |E_0^{\text{p}}(M, L)/M|$  from the BTCSA approximation to the partition function, and compared it with the result obtained directly by using the TCSA for a circle. The result should be independent of the boundary conditions, and that is indeed what we found. The results are given in figure 2a, in which we compare the direct TCSA (or TBA) evaluation of  $\log |E_0^{\text{p}}(M, L)/M|$  for the model on a circle (solid line) with the result obtained from the BTCSA evaluation of  $Z_{\mathbb{1}\Phi(0)}$  with a truncation to 29 states (points), and of  $Z_{\mathbb{1}\mathbb{1}}$  with a truncation to 26 states (open circles). As can be seen, the values for  $E_0^{\text{p}}(M, L)/M$  obtained via the BTCSA are indeed independent of the boundary conditions on the strip, and agree with the expected answers obtained by looking directly in the other channel.

For our second example we estimated the ground state degeneracy functions  $\log(g_{\alpha}(M, L)g_{\beta}(M, L))$  for  $(\alpha, \beta)$  taking the two values  $(\mathbb{1}, \mathbb{1})$  and  $(\mathbb{1}, \Phi(0))$ . The BTCSA calculations are rather more sensitive to truncation error than in the previous example, and we took results from various truncations up to 98 states, and then extrapolated in the truncation level. The numerical results at  $(ML) = 0.02$  are compared with the exact results at  $L = 0$  in table 1.

We also performed a more detailed investigation of  $\log(g_{\mathbb{1}}(M, L)g_{\mathbb{1}}(M, L))$ , and  $\log(g_{\mathbb{1}}(M, L)g_{\Phi(h)}(M, L))$ . These should both flow from their UV values in table 1 to IR values of 0; but whereas there is a single flow for the  $(\mathbb{1}, \mathbb{1})$  boundary conditions,  $\log(g_{\mathbb{1}}(M, L)g_{\Phi(h)}(M, L))$  depends on the dimensionless parameter  $hM^{-6/5}$ . For



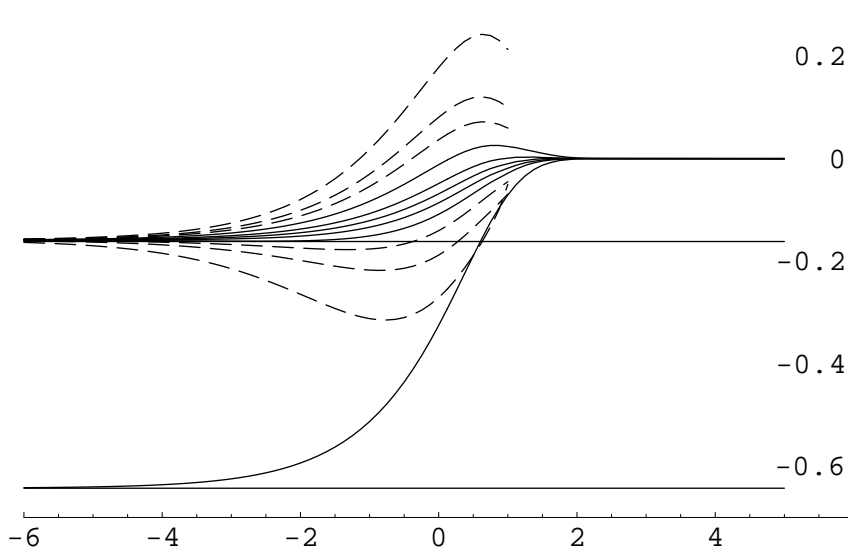
2a)  $\log |E_0^p(M, L)/M|$  plotted against  $\log(ML)$  for the SLYM on a circle: TCSA for the system on a circle (line) compared with results from the BTCSA with boundary conditions  $(\mathbb{1}, \Phi(0))$  (points) and  $(\mathbb{1}, \mathbb{1})$  (circles).

The b.c.s $(\alpha, \beta)$	The exact value of $\log(g_\alpha(M, 0) g_\beta(M, 0))$	The BTCSA estimate for $\log(g_\alpha(M, \frac{0.02}{M}) g_\beta(M, \frac{0.02}{M}))$
$(\mathbb{1}, \mathbb{1})$	$\frac{1}{2} \log((5-\sqrt{5})/10) = -0.64296\dots$	$-0.643 \pm 0.001$
$(\mathbb{1}, \Phi(0))$	$\frac{1}{2} \log((5+\sqrt{5})/10) = -0.161754\dots$	$-0.1616 \pm 0.0005$

Table 1: the BTCSA estimates and exact values of  $\log(g_\alpha(M, 0) g_\beta(M, 0))$

small  $|hM^{-6/5}|$  this should still leave essentially a single crossover region from  $(\mathbb{1}, \Phi)$  conformal boundary conditions in the UV to massive boundary conditions in the IR, but we should expect that for large  $hM^{-6/5}$  there are two crossover regions – first a massless boundary flow at  $Lh^{5/6} \sim 1$  from the  $(\mathbb{1}, \Phi)$  CBCs in the UV to effective  $(\mathbb{1}, \mathbb{1})$  CBCs, and then a crossover from these CBCs to the IR boundary conditions which should agree with the single crossover for the true  $(\mathbb{1}, \mathbb{1})$  case.

In figure 2b we give plots of these functions against  $\log(ML)$  for various values of  $(hM^{-6/5})$ . The two straight lines in this plot are the exact UV values from table 1. The lowermost curve is  $\log(g_{\mathbb{1}}(M, L) g_{\mathbb{1}}(M, L))$  from BTCSA at 43 states, showing a smooth flow from the UV value  $-0.64\dots$  to the IR value 0. The remaining curves are  $\log(g_{\mathbb{1}}(M, L) g_{\Phi(h)}(M, L))$  from BTCSA at 36 states. The values of  $hM^{-6/5}$ , starting with the uppermost line and ending with the lowest line, are  $-0.65, -0.5, -0.4, -0.25, -0.1, 0, 0.1, 0.25, 0.5, 1.0,$  and  $3.0$  respectively.



2b)  $\log(g_{\parallel}(M, L) g_{\parallel}(M, L))$  and  $\log(g_{\parallel}(M, L) g_{\Phi(h)}(M, L))$  plotted against  $\log(ML)$  for various values of  $(hM^{-6/5})$ ; details given in the text. Also shown are the exact UV values from table 1.

There was one problem in finding numerical values for  $\log(g_{\parallel}(M, L) g_{\Phi(h)}(M, L))$ , and this was estimating  $B_{\alpha\beta} L$ . It is only for large values of  $ML$  that equation (3.7) holds, and for large values of  $|hM^{-6/5}|$  this is outside the region of convergence of the BTCSA method. We were only able to find  $B_{\parallel\Phi(h)} L$  directly from equation (3.7) for  $|hM^{-6/5}| \lesssim 0.1$ ; for the remaining values of  $hM^{-6/5}$ , we estimated  $B_{\parallel\Phi(h)} L$  by extrapolation of the data for  $|hM^{-6/5}| \leq 0.0125$ .

To mark this loss of accuracy, for  $-0.25 \leq (hM^{-6/5}) \leq 0.25$  we have plotted  $\log(g_{\parallel}(M, L) g_{\Phi(h)}(M, L))$  for  $-6 < \log(ML) < 5$  with solid lines, but for the remaining values of  $(hM^{-6/5})$  we have only given results for  $\log(ML) < 1$ , and used dashed lines. We estimate the error in  $\log(g_{\parallel}(M, L) g_{\Phi(h)}(M, L))$  at  $ML = 1$  arising from the extrapolation of  $B_{\parallel\Phi(h)} L$  to be of the order of 0.01% for  $(hM^{-6/5}) = 0.3$ , rising to 20% for  $(hM^{-6/5}) = 3.0$ . For larger values of  $(hM^{-6/5})$  the errors in extrapolation render our data meaningless.

For small values of  $|hM^{-6/5}|$  (less than about 0.3), we expect our results to be quite accurate. While the quantitative results are less good for the larger values, we do still believe that there is good qualitative agreement. We now comment on the results in figure 2b. There are essentially three different behaviours shown in this figure.

1. For  $|hM^{-6/5}| \sim 0$  we found a single crossover to the massive case, with only

small deviations due to the boundary field.

2. For  $(hM^{-6/5}) \gtrsim 1.0$ , we found clear signs of two crossover regions as  $L$  varied from 0 to  $\infty$ : the first (for small  $L$ ) a massless boundary flow from the value with  $(\mathbb{1}, \Phi(0))$  b.c.s to that with  $(\mathbb{1}, \mathbb{1})$  b.c.s, and then a second region (for larger  $L$ ) with a crossover to zero as the bulk mass scale dominates. We were not able to go to large enough values of  $(hM^{-6/5})$  to truly separate the two crossover regions, but we think that figure 2b is very suggestive of the behaviour we propose.
3. For some value of  $(hM^{-6/5})$  between  $-0.8$  and  $-0.6$ , there is a critical value at which  $\log(g_{\mathbb{1}}(M, L) g_{\Phi(h)}(M, L))$  diverges – this was signalled by a pole in a rational fit to the data for  $B_{\mathbb{1}\Phi(h)} L$  for small  $|hM^{-6/5}|$ . The predicted position of this pole is in agreement with the critical value  $(h_{\text{crit}} M^{-6/5}) = -0.68529$  discussed, from a different point of view, at the end of section 6 below.

## 4 Boundary TBA

For the rest of this paper we restrict our attention to cases where the bulk is massive, so that the bulk S-matrix is known. In situations where boundary reflection factors are also known (or conjectured), TBA-like equations for the ground-state energy on an interval have been put forward in refs. [6, 7]. The derivation of these equations begins with the expression given in [1] for the boundary state  $|B_\alpha\rangle$  corresponding to the boundary condition  $\alpha$ :

$$|B_\alpha\rangle = \exp \left[ \int_{-\infty}^{\infty} d\theta K_\alpha(\theta) A(-\theta) A(\theta) \right] |0\rangle, \quad (4.1)$$

where  $K_\alpha(\theta)$  is related to the reflection factor for the  $\alpha$  boundary condition by  $K_\alpha(\theta) = R_\alpha(\frac{i\pi}{2} - \theta)$ , and  $A(\theta)$  (denoted  $A^\dagger(\theta)$  in [7]) is the Faddeev-Zamolodchikov operator creating a single particle with rapidity  $\theta$ . (As in [7], we ignore the possible presence of additional zero-momentum particles in this state. At least in some regimes, this will be retrospectively justified via a comparison with BTCSA data.)

The next step is to express the partition function  $Z_{\alpha\beta}(M, R, L)$  of the model on a cylinder of length  $R$  and circumference  $L$  as

$$Z_{\alpha\beta}(M, R, L) \sim {}_L\langle B_\alpha | \exp(-RH_p(M, L)) | B_\beta \rangle_L \quad (4.2)$$

where  $H_p(M, L)$  is the Hamiltonian for the system living on a circle of circumference  $L$ , with periodic boundary conditions and bulk mass  $M$ , and  $|B_\alpha\rangle_L$  and  $|B_\beta\rangle_L$  are boundary states set up as in (4.1), but on the circle rather than the infinite line. Expanding the expressions for these states and then making a saddle-point approximation (bearing in mind the quantisation conditions imposed on the momenta by the periodic boundary conditions) ultimately leads to an expression for

$-(\log Z_{\alpha\beta}(M, R, l/M))/l$  which becomes exact in the limit  $l \rightarrow \infty$ . But in this limit – the opposite to that considered in the discussion following equation (3.6) – the same quantity is given as  $E_0^{\alpha\beta}(M, R)$ , the sought-after ground-state energy of  $H_{\alpha\beta}(M, R)$ . The calculational details can be found in ref. [7]; the upshot is that  $E_0^{\alpha\beta}(M, R)$  is expressed in terms of the solution  $\varepsilon(\theta)$  to the following nonlinear integral equation:

$$\varepsilon(\theta) = 2r \cosh \theta - \log \lambda_{\alpha\beta}(\theta) - \phi * L(\theta) \quad (4.3)$$

where  $r = MR$ ,  $L(\theta) = \log(1 + e^{-\varepsilon(\theta)})$ ,  $f * g(\theta) = \frac{1}{2\pi} \int_{-\infty}^{\infty} d\theta' f(\theta - \theta') g(\theta')$ , and

$$\lambda_{\alpha\beta}(\theta) = K_{\alpha}(\theta) K_{\beta}(-\theta), \quad \phi(\theta) = -i \frac{\partial}{\partial \theta} \log S(\theta), \quad (4.4)$$

with  $S(\theta)$  the bulk S-matrix (2.6), and  $M$  is the particle mass (2.7). The solution to (4.3) for a given value of  $r$  (and of any boundary-related parameters hidden inside the labels  $\alpha$  and  $\beta$ ) determines a function  $c(r)$ :

$$c(r) = \frac{6}{\pi^2} \int_{-\infty}^{\infty} d\theta r \cosh \theta L(\theta) \quad (4.5)$$

in terms of which  $E_0^{\alpha\beta}(M, R)$  (which from here on we abbreviate to  $E_0(R)$ , when there is no danger of confusion) is

$$E_0(R) = E_{\text{bdry}} + \mathcal{E}_{\text{bulk}} R - \frac{\pi}{24R} c(MR), \quad (4.6)$$

where  $E_{\text{bdry}}$  is a possible constant contribution to  $E_0(R)$  coming from the boundaries, and  $\mathcal{E}_{\text{bulk}}$  is the bulk energy per unit length. We will also be working with a dimensionless ground state scaling function  $F(r)$ . With the bulk mass now nonzero, the discussion of BTBA results is most convenient if this is used to set the overall length scale, rather than the boundary magnetic field used in the definition (3.3) of the last section. Thus we set

$$F(r) = \frac{R}{\pi} E_0(R) = \frac{r}{\pi M} E_{\text{bdry}} + \frac{r^2}{\pi M^2} \mathcal{E}_{\text{bulk}} - \frac{1}{24} c(r). \quad (4.7)$$

The equations (4.3)–(4.5) are superficially very similar to the more familiar TBA equations found for periodic boundary conditions, but there are some important new features, as we now show. The identity  $\lambda_{\alpha\beta}(\theta - i\pi/3) \lambda_{\alpha\beta}(\theta + i\pi/3) = \lambda_{\alpha\beta}(\theta)$  (which follows from the boundary bootstrap equations for the scaling Lee-Yang model) is enough to establish that the function  $Y(\theta) = \exp(\varepsilon(\theta))$  solves the same  $Y$ -system as found in the standard Lee-Yang TBA, namely [20]

$$Y(\theta - i\pi/3) Y(\theta + i\pi/3) = 1 + Y(\theta). \quad (4.8)$$

From there, the standard periodicity property  $Y(\theta + 5i\pi/3) = Y(\theta)$  follows by simple substitution. However the consequent  $r$ -dependence of the solutions is different,

because the  $\lambda_{\alpha\beta}(\theta)$  term in (4.3) gives the function  $\varepsilon(\theta)$  a non-trivial behaviour near  $\theta = 0$ , and this persists even in the  $r \rightarrow 0$  limit. The limiting shape of  $\varepsilon(\theta)$  is a pair of ‘kink’ regions near to  $\theta = \pm \log(1/r)$ , separated by two plateaux from what might fancifully be called a ‘breather’ region near to  $\theta = 0$ . (This is in contrast to the situation in the usual TBA where there are just the two kink regions at  $\theta \approx \pm \log(1/r)$ , separated by a single plateau of length  $2 \log(1/r)$  [5].) As explained in [20], the  $r$ -dependence of the ultraviolet-limiting solutions creeps in via interactions between the regions where the  $\theta$ -dependence of  $\varepsilon(\theta)$  remains non-trivial, and here these are separated by a distance  $\log(1/r)$ , *half* the value found for periodic boundary conditions. As a result, the regular part of the expansion of  $c(r)$  is generically a power series in  $r^{6/5}$ , rather than the  $r^{12/5}$  that is found when the boundary conditions are periodic.

The other, ‘irregular’, parts of the function  $c(r)$  can be traced to the integral against  $r \cosh \theta$  in (4.5). The mechanism is as described in [5], though the arguments must be generalised to incorporate the effect of the central breather region. If, in terms of the blocks  $(x)$  defined in equation (2.6), the reflection factors  $R_{\alpha/\beta}$  are equal to  $\prod_{x \in A_{\alpha/\beta}} (x)$ , then the final result is that

$$c(r) = \frac{4\sqrt{3}}{\pi} \left( \sum_{x \in A_{\alpha} \cup A_{\beta}} \sin \frac{x\pi}{3} \right) r - \frac{2\sqrt{3}}{\pi} r^2 + \text{‘regular terms’}, \quad (4.9)$$

where ‘regular terms’ refers to the already-discussed power series in  $r^{6/5}$ . As will be justified via a specific example in the next section, the scaling function  $F(r)$  is expected to expand in powers of  $r^{6/5}$  alone about  $r = 0$ . This will be reproduced by the BTBA result of (4.7) and (4.9), so long as the irregular terms in (4.9) cancel against the explicit bulk and boundary energies included in (4.7). This requirement determines the constants  $\mathcal{E}_{\text{bulk}}$  and  $E_{\text{bdndry}}$  exactly:

$$E_{\text{bdndry}} = \frac{1}{2\sqrt{3}} \left( \sum_{x \in A_{\alpha} \cup A_{\beta}} \sin \frac{x\pi}{3} \right) M \quad ; \quad \mathcal{E}_{\text{bulk}} = -\frac{1}{4\sqrt{3}} M^2. \quad (4.10)$$

The value of  $\mathcal{E}_{\text{bulk}}$  is the same as is found when the boundary conditions are periodic [5]. This is as it should be, since  $\mathcal{E}_{\text{bulk}}$  reflects a bulk property of the model.

Finally we remark that the driving term in (4.3),  $2r \cosh \theta - \log \lambda_{\alpha\beta}(\theta)$ , is singular at the poles and zeroes of  $\lambda_{\alpha\beta}(\theta)$ . Therefore a set of  $r$ -independent points at which  $Y(\theta)$  either vanishes or is infinite can be read directly off (4.3), at least in the strip  $-\pi/3 \leq \text{Im} \theta \leq \pi/3$ <sup>†</sup>. Points of the first sort, at which  $L(\theta)$  is also singular, are also seen in solutions of more usual TBA equations; they were called ‘type II’ in [21]. Those of the second sort are a new feature of the boundary TBA, and will be dubbed ‘type III’.

---

<sup>†</sup>beyond this strip, the  $Y$ -system relation (4.8) should be used.

## 5 The $(\mathbb{1}, \Phi(h))$ ground state in the BTBA

We can now discuss the physical import of these results, with particular reference to the strip with  $(\mathbb{1}, \Phi(h))$  boundary conditions mentioned in section 3. For this setup the Hamiltonian (3.1) has  $\phi_L = 0$ ,  $2-x_\varphi = 12/5$ , and  $1-x_R = 6/5$ . Therefore, the conformal perturbation theory expansion of  $F(r)$  does have a regular expansion in  $r^{6/5}$ , and so matches the behaviour derived in the last section within the BTBA.

Next, we should decide which reflection factors describe the  $(\mathbb{1}, \Phi(h))$  situation. We found that substituting  $\lambda_{\alpha\beta}(\theta) = K_{(1)}(-\theta)K_b(\theta)$  into the basic BTBA equation (4.3) enabled us to reproduce BTCSA data for  $-0.68529 < h < 0.554411$ , the necessary values of  $b$  lying in the range  $-2 \leq b \leq 2$ . The natural conclusion, which will receive further support from its consistency with results to be reported in the remainder of this paper, is to associate boundary conditions with reflection factors as follows:

$$\mathbb{1} \leftrightarrow R_{(1)}(\theta) \quad (5.1)$$

$$\Phi(h) \leftrightarrow R_b(\theta) \quad (5.2)$$

The precise relation between  $h$  and  $b$  will be discussed shortly, but in terms of  $b$  the constant part of  $E_0(R)$  at large  $R$  now follows from the general result (4.10), and is:

$$E_{\text{bdry}} = \frac{1}{2} \left( \sqrt{3} - 1 + 2 \sin \frac{b\pi}{6} \right) M . \quad (5.3)$$

Our numerical work with this particular  $\lambda_{\alpha\beta}(\theta)$  was complicated by the presence, for  $-2 < b < 2$ , of a double type II singularity in  $L(\theta)$  at  $\theta=0$ . (At  $b=-2$  there is no singularity, and at  $b=2$  it is of order 4.) Therefore, in the general case  $e^{-\varepsilon(\theta)}$  is singular at  $\theta=0$ , and the direct numerical integration of equation (4.3) gives very unsatisfactory results: we estimated the accuracy for  $c(r)$  at small  $r$  to be between  $10^{-2}$  and  $10^{-3}$ . To alleviate this problem we defined

$$\widehat{\varepsilon}(\theta) = \varepsilon(\theta) - q \log \tanh \frac{3}{4}\theta + \log \widehat{\lambda}_{\alpha\beta}(\theta) \quad , \quad \widehat{L}(\theta) = \log \left( \tanh^q \frac{3}{4}\theta + \widehat{\lambda}_{\alpha\beta}(\theta) e^{-\widehat{\varepsilon}(\theta)} \right) \quad (5.4)$$

where  $q$  is the order of the pole at the origin (0, 2 or 4),

$$\widehat{\lambda}_{\alpha\beta}(\theta) = \lambda_{\alpha\beta}(\theta) \left( \frac{S(\theta - i\pi/3)}{S(\theta + i\pi/3)} \right)^{q/2} \quad , \quad (5.5)$$

and  $\alpha = (1)$ ,  $\beta = b$  for this particular case. (The motivation for these redefinitions came from analogous manoeuvres performed in refs. [8, 21] for certain excited-state TBA equations for periodic boundary conditions.) Equations (4.3) and (4.5) can then be recast in the following form:

$$\widehat{\varepsilon}(\theta) = 2r \cosh \theta - \phi * \widehat{L}(\theta) \quad , \quad c(r) = \frac{12\sqrt{3}}{\pi} qr + \frac{6}{\pi^2} \int_{-\infty}^{\infty} d\theta r \cosh \theta \widehat{L}(\theta) \quad (5.6)$$

These revised equations are nonsingular on the real axis, and so can be solved numerically with higher accuracy.

The attempt to go beyond the range  $-2 < b < 2$  exposes a couple of subtleties of the boundary TBA. We start with the situation as the point  $b = -2$  is approached. A study of the singularities of  $L(\theta)$  in the complex  $\theta$ -plane revealed a pair of  $Y(\theta) = -1$  ('type I' in the language of [21]) singularities on the imaginary axis, at  $\theta = \pm\theta_p$  say. They are confined to the segment  $0 < |\text{Im}\theta_p| < (b+2)\pi/6$  by the double type II singularity at the origin, and type III singularities at  $\pm i(b+2)\pi/6$ . As  $b$  approaches  $-2$  from above, the length of this segment shrinks to zero and the points  $\pm\theta_p$  are forced towards the origin. In order to continue round  $-2$  to smaller real values of  $b$ , a deformation of integration contours is therefore required. This is just as occurs during the analytic continuation (in  $r$ ) of ordinary TBA equations, discussed in refs. [9,21]. When the deformed contours are returned to the real  $\theta$ -axis, residue terms are picked up [9], and the singularities at  $\pm\theta_p$  become 'active', in that their positions appear explicitly in the analytically-continued equations. These equations are:

$$\varepsilon(\theta) = 2r \cosh \theta - \log \lambda_{(1)b}(\theta) + \log \frac{S(\theta - \theta_p)}{S(\theta + \theta_p)} - \phi * L(\theta), \quad (5.7)$$

$$c(r) = \frac{6}{\pi^2} \int_{-\infty}^{\infty} d\theta r \cosh \theta L(\theta) + i \frac{24r}{\pi} \sinh \theta_p. \quad (5.8)$$

As in [9], we adopt the convention that  $\theta_p$  has a positive imaginary part *after* the real  $\theta$  axis has been crossed, and the corresponding singularity has become active. Its precise value appears as a free parameter in the equations, and must be fixed by imposing

$$\varepsilon(\theta_p) = i\pi. \quad (5.9)$$

These equations describe the ground state, for all real  $r$ , whenever  $b$  is in the interval  $-4 < b < -2$ . As before, the redefinitions (5.4) can be used to put the equations into a form better suited to numerical work.

At  $b=2$ , a different phenomenon occurs: two (inactive) type II singularities, at  $\pm i(b-2)\pi/6$ , hit the real  $\theta$  axis. As explained in section 3.4 of ref. [21], when in the standard TBA the real  $\theta$  axis is crossed by type II singularities, the continued equations can always be recast into the form that they had before the crossing, although in general some of the active singularities may have to be relocated from their analytically-continued positions. The same is true here, and the mechanism is as follows. After the point  $b=2$ , the singularities at  $\pm i(b-2)$  are active and the initial analytic continuation of the basic BTBA equation (4.3) is therefore

$$\varepsilon(\theta) = 2r \cosh \theta - \log \lambda_{(1)b}(\theta) - \log \frac{S(\theta - i(b-2)\pi/6)}{S(\theta + i(b-2)\pi/6)} - \phi * L(\theta). \quad (5.10)$$

Equation (5.7) arose in just the same way, though there was a different sign for the extra term, because of the opposite signs of the residues for type I and type II



singularities. This time there is no need for an equivalent of equation (5.9), since the relevant singularities owe their existence to the factor  $\lambda_{(1)b}(\theta)$  and so, as mentioned at the end of section 4, their positions are fixed irrespective of any other details of the solution. Now the identity

$$K_b(\theta) \frac{S(\theta - i(b-2)\pi/6)}{S(\theta + i(b-2)\pi/6)} = K_{4-b}(\theta) \quad (5.11)$$

can be used to rewrite the analytically-continued equation as

$$\varepsilon(\theta) = 2r \cosh \theta - \log \lambda_{(1)4-b}(\theta) - \phi * L(\theta). \quad (5.12)$$

As promised, this has the same form as the basic BTBA equation (4.3), which applied before the point  $b=2$  was passed, the only change being that the parameter  $b$  has been replaced by  $4-b$ . It is straightforward to check that the expression (4.5) for  $c(r)$  behaves in an analogous fashion under the continuation, and so the system of equations has a (somewhat hidden) symmetry about  $b=2$ . Furthermore, as described in a related context in [21], there is no reason for the  $b$ -dependence to be in any way singular at this point: it is best thought of as a ‘coordinate singularity’, with the apparently discontinuous behaviour residing solely in the BTBA equations, and not in the functions  $Y$  and  $c$  that they encode. If the original equations had been rewritten using contours shifted away from the real  $\theta$  axis for all integrations, then the same functions would have been recovered, but from a system for which the point  $b=2$  had no special status.

Combining the symmetry about  $b=2$  with the evident symmetry of the equations about  $b=-3$  leads to the conclusion that the ground-state BTBA is periodic in the parameter  $b$  with period 10. This might be a little surprising, since from (2.9) the periodicity in  $b$  of the driving term  $\lambda_{(1)b}(\theta)$  itself is 12, but is well confirmed by our numerical results. Consider now the ‘regular’ part of  $c$ , a function of  $b$  and  $r$  with an expansion in powers of  $r^{6/5}$ . By the result just established, each coefficient in this expansion must be a periodic function of  $b$  with period 10. An excellent numerical fit for the first coefficient turns out to be  $-5.1041654269(9) \sin((b+0.5)\pi/5)$  (remarkably, all higher modes allowed by the periodicity appear to be absent). This coefficient can also be found in terms of  $h$ , and is equal to  $24\Gamma(2/5)^{1/2} \Gamma(6/5)^{1/2} \Gamma(4/5)^{-1} (\pi M)^{-6/5} h = 1.6794178 M^{-6/5} h$ .

Combining the two expressions yields the relation between  $b$  and  $h$ :

$$h(b) = -0.685289983(9) \sin\left((b+0.5)\pi/5\right) M^{6/5}. \quad (5.13)$$

With  $h(b)$  given by this formula we found an excellent numerical agreement between the BTBA and BTCSA data at all real values of  $b$ . A particularly striking check came on setting  $b=-0.5$ : from (5.13), this should correspond to the ‘pure’  $\Phi$  boundary condition, with no boundary field, and should therefore have an expansion in powers

of  $r^{12/5}$ . Thus *all* odd powers of  $r^{6/5}$  (and not just the first) should vanish in the regular expansion of  $c(r)$  at this point, and within our numerical accuracy that is indeed what we found:

$$\begin{aligned} c(r)|_{b=-0.5} &= 0.4 + \frac{6(\sqrt{3}-1)(2-\sqrt{2})}{\pi} r - \frac{2\sqrt{3}}{\pi} r^2 \\ &\quad - 8.18 \times 10^{-12} r^{6/5} + 0.554031116 r^{12/5} \\ &\quad + 1.14 \times 10^{-9} r^{18/5} - 0.0025228 r^{24/5} - 2.88 \times 10^{-7} r^6 + \dots \end{aligned} \quad (5.14)$$

## 6 The generalisation to excited states

We now turn to the excited states. In principle, the analytic continuation method of [9] can be used to derive the relevant generalisations of the basic BTBA equations. We have yet to complete this in detail, but knowledge of the method allowed us to make an educated guess as to the form that the equations would take, which we then verified by means of a direct comparison with BTCSA data. For the one-particle states on the strip, the equations turned out to have the same form as those found in [9] for *two*-particle states on a circle. With  $(\mathbf{1}, \Phi(h))$  boundary conditions they are:

$$\varepsilon(\theta) = 2r \cosh \theta - \log \lambda_{(1)b}(\theta) + \log \frac{S(\theta - \theta_0)}{S(\theta - \bar{\theta}_0)} + \log \frac{S(\theta + \theta_0)}{S(\theta + \bar{\theta}_0)} - \phi * L(\theta), \quad (6.1)$$

$$c(r) = \frac{6}{\pi^2} \int_{-\infty}^{\infty} d\theta r \cosh \theta L(\theta) + i \frac{24r}{\pi} (\sinh \theta_0 - \sinh \bar{\theta}_0), \quad (6.2)$$

$$\varepsilon(\theta_0) = (2n+1)\pi i, \quad \varepsilon(\bar{\theta}_0) = -(2n+1)\pi i, \quad (6.3)$$

where, as before,  $\lambda_{(1)b}(\theta) = K_{(1)}(\theta)K_b(-\theta)$ . As in the last section, we desingularised these equations before studying them numerically. For real  $r$ ,  $\bar{\theta}_0$  is equal to  $\theta_0^*$ , the complex conjugate of  $\theta_0$ , and so only one of the conditions (6.3) needs to be imposed. This is the generic form of the equations for  $-2 < b < 2$ .

For levels for which the one-particle excited-state equations retain the form of (6.1)–(6.3) as  $r \rightarrow \infty$ , a large- $r$  asymptotic can be extracted much as in [8, 9]. The result is

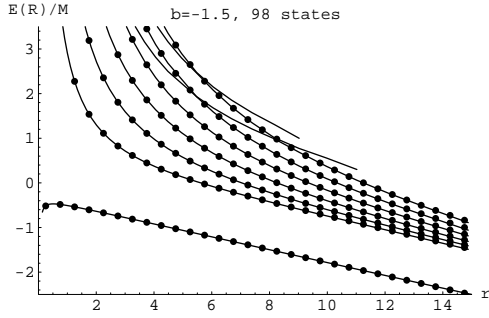
$$E(R) - E_0(R) = M \cosh \beta_0 \quad (6.4)$$

where  $\beta_0 = \text{Re}(\theta_0)$  satisfies

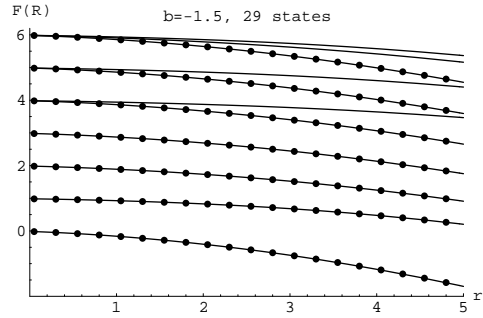
$$2r \sinh \beta_0 - i \log R_{(1)}(\beta_0)R_b(\beta_0) = 2\pi k, \quad (6.5)$$

and the value of the integer  $k$  is fixed by a combination of the quantisation condition (6.3) and the sign of  $(\text{Im}(\theta_0) - \pi/6)$ :

$$k = 2n + \frac{1}{2}(1 - \text{sign}(\text{Im}(\theta_0) - \pi/6)). \quad (6.6)$$



3a) Energy levels  $E(R)/M$  plotted against  $r$  for the  $(\mathbb{1}, \Phi(h))$  boundary conditions, with  $b=-1.5$ ,  $h=0.402803 M^{6/5}$ . BTBA results (points) compared with the BTCSA (lines).



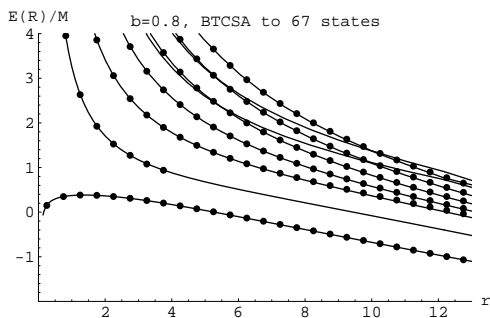
3b) The same as figure 3a, but showing the scaling functions  $F(r)$  to exhibit the ultraviolet behaviour.

Equation (6.5) is just the ‘boundary Bethe ansatz’ (BBA) quantisation condition for the rapidity  $\pm\beta_0$  of a single particle bouncing between the two ends of the interval. Further analytic results can be obtained, but for the rest of this section we will instead discuss some general features that emerge as  $b$  is varied.

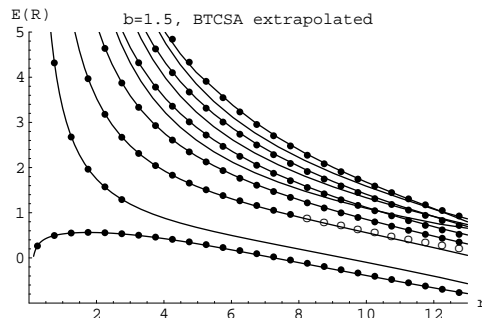
For  $b$  in the range  $-4 < b < -2$ , a manoeuvre similar to that seen in the last section for the ground state in the same region appears to be necessary, resulting in the appearance of a further pair of active singularities in the system, situated on the imaginary axis. Even for real  $r$ , there are then two independent singularity positions to be fixed, making the equations harder to handle numerically. We therefore leave this regime to one side for the time being, and move on to the range  $-2 < b < -1$ . In this regime, the basic one-particle equations (6.1)–(6.3) hold for all real  $r$ , for all one-particle levels. Figures 3a and 3b compare BTBA results (points) with the first few levels found using the BTCSA (continuous lines), at  $b = -1.5$ ,  $h=0.402803 M^{6/5}$ . Notice that the plotted points do not cover all of the lines visible on the figure: those missed correspond to states containing more than one particle in the infrared, and are presumably described by BTBA systems with more active singularities than the four (at  $\pm\theta_0$  and  $\pm\bar{\theta}_0$ ) present in (6.1)–(6.3).

As  $b$  passes  $-1$ , the lowest excited state as seen in plots of BTCSA data breaks away from the other excited levels and dips below the one-particle threshold. Physically the reason for this is clear: at  $b=-1$  an extra pole in  $R_b(\theta)$  enters the physical strip, signalling the appearance of a boundary bound state. After this point the infrared behaviour of this level changes from that of a free particle bouncing between the two boundaries to that of a particle trapped near to the  $\Phi(h)$  boundary, a state with asymptotic gap  $M\cos((b+1)\pi/6)$ . All of this can be seen in the BTCSA data, with the value of  $b$  related to  $h$  via (5.13). Since  $h(b)$  had previously been obtained by a matching of data in the ultraviolet, this infrared agreement provides a nontrivial

check on the consistency of our results.



4) Energy levels  $E(R)/M$  plotted against  $r$  for  $b=0.8$ ,  $h=-0.499555 M^{6/5}$ . Labelling as in figure 3a.



5) Energy levels  $E(R)/M$  plotted against  $r$  for  $b=1.5$ ,  $h=-0.65175 M^{6/5}$ . Labelling as in figure 3a, with BBA results plotted as ( $\circ$ ).

Figure 4 shows the situation at  $b=0.8$ ,  $h=-0.499555 M^{6/5}$ , by which stage the dip in the first level has become quite pronounced. The points on the graph show BTBA results found using (4.3) and (6.1)–(6.3), and it will be observed that the lowest set of excited points stops short. (The other sets persist to  $r=\infty$  and for these the derivation of the BBA asymptotic (6.4) is valid.) At  $r \approx 4$ , the basic excited-state BTBA (6.3) for the first excited level breaks down, with an initial transition similar to that observed in [21] for the second excited state of the  $T_2$  model. This reflects the fact that the particle is becoming bound to the  $\Phi(h)$  boundary. The BTBA equations become more complicated in this regime, and we postpone their detailed study to future work. However in some regimes preliminary predictions can be obtained, in the spirit of [22], by supposing that solutions to the BBA equation (6.5) can be continued to complex values of  $\beta_0$ . This amounts to approximating the problem by the quantum *mechanics* of a single particle reflecting off the two walls with amplitudes  $R_{(1)}$  and  $R_b$ . For  $-1 < b < 0$ , the first excited level as found from the BTCSA can be modelled with reasonable accuracy by a solution  $\beta_0(r)$  to the BBA which starts off real at small  $r$ , reaches zero at some ( $b$ -dependent) point  $r_c$ , and then becomes purely imaginary, tending to  $i(b+1)\pi/6$  from below as  $r$  tends to infinity. However for  $b > 0$  the only candidate solution is satisfactory at best only for large  $r$ , which is why such points have been omitted from figure 4. (The relevant  $\beta_0(r)$  tends to  $i(b+1)\pi/6$  from above at large  $r$ , implying an approach to the asymptotic mass gap from below rather than above, but our large- $r$  BTCSA data is not yet precise enough to check on this prediction.)

Continuing to increase  $b$ , the next development occurs at  $b=1$ ,  $h=-0.554411 M^{6/5}$ , where a second excited level starts to drop below threshold, this time tending to a gap of  $M\cos((b-1)\pi/6)$  as  $R \rightarrow \infty$ . This heralds the arrival of a second boundary bound state pole in  $R_b(\theta)$  onto the physical strip. Figure 5 shows the situation for

$b=1.5$ . For this value of  $b$ , the predicted dip in the second excited level is rather small (about  $0.03M$ ) and is only seen at rather large values of  $R$ , where the BTCSA is at the limits of its useful range. A more accurate reflection of the infrared behaviour of this second excited level is probably provided by the analytically-continued BBA solution plotted on the figure as open circles. The BTBA equations (6.3) now break down for both the first and the second excited levels, at  $r \approx 4$  and  $r \approx 9$  respectively.

Finally, at  $b=2$ ,  $h=h_{\text{crit}}=-0.68529M^{6/5}$ , the asymptotic mass gap of the lowest excited state hits zero. It is not possible to increase  $h$  any further without making  $b$  complex; if a larger value is used in the BTCSA then we find energy levels becoming complex at large  $r$ . This can be seen analytically by combining (5.13) and (5.3) to write  $E_{\text{bdry}}$  as a function of  $h$ : a square-root singularity is revealed at  $h=h_{\text{crit}}$ , matching perfectly behaviour that can be seen directly in the BTCSA. Presumably, the boundary perturbation has destabilised the bulk vacuum, a situation that will most probably repay further study.

## 7 Other combinations of boundary conditions

Consideration of the strip with  $(\mathbb{1}, \Phi(h))$  boundary conditions has sufficed to establish the key relation (5.13), and has also enabled us to check on the basic consistency of our associations (5.1) and (5.2) of the reflection factors  $R_{(1)}$  and  $R_b$  with the  $\mathbb{1}$  and  $\Phi(h(b))$  boundary conditions. However, it is natural to wonder how the two other possible pairs of boundary conditions can be described, and this is the topic of this section.

First, to the  $(\mathbb{1}, \mathbb{1})$  situation. From the identifications made earlier, one might expect that ground state would be described by the basic BTBA system (4.3), with  $\lambda_{\alpha\beta}(\theta) = K_{(1)}(\theta)K_{(1)}(-\theta)$ . However, a calculation of the ultraviolet central charge as in [7] yields the answer  $c(0) = 2/5$ , instead of the  $-22/5$  expected on the basis of the conformal result (3.2). Moreover, numerical comparisons of BTBA and BTCSA results show no agreement. To motivate the resolution of this problem, we recall from section 3 that the  $\mathbb{1}$  boundary condition can be obtained from the  $\Phi(h)$  boundary condition by sending  $h$  to  $+\infty$ . That was with the bulk massless, but if we consider an interval of length  $R$  with  $(\mathbb{1}, \Phi(h))$  boundary conditions and take the  $+h/M^{6/5} \rightarrow \infty$  limit while keeping  $R$  of the same order as the bulk scale  $1/M$ , then it should be possible (after suitable renormalisations) to arrive at the correct BTBA. We hope to say more about this elsewhere, but for now we just observe, from (5.13), that at the level of the BTBA the desired continuation will be found on setting  $b = -3 + i\hat{b}$ , and then varying  $\hat{b}$  from zero to infinity. The starting-point for this continuation lies in the  $-4 < b < -2$  regime of the  $(\mathbb{1}, \Phi(h))$  ground-state BTBA, and is hence described by the modified system (5.7)–(5.9). This observation gave us the hint that the  $(\mathbb{1}, \mathbb{1})$  ground state might also be described by a BTBA system in which two singularities are already active. We therefore returned to the numerical study of the modified

equations (5.7)–(5.9), this time with  $\lambda_{\alpha\beta}(\theta) = K_{(1)}(\theta)K_{(1)}(-\theta)$ . The BTCSA data for the  $(\mathbb{1}, \mathbb{1})$  ground state was matched perfectly over the full range of  $r$ , with a behaviour that is very similar to that of the first excited-state TBA for the SLYM on a circle [8, 9]. The equations exhibit a single transition between an infrared regime, where two active singularities lie on the imaginary  $\theta$  axis, and an ultraviolet regime where these are split and join the kink systems at  $\theta \approx \pm \log(1/MR)$ . As a result, each of these kink systems has a type II singularity sitting on the real  $\theta$  axis, a fact which modifies the predicted value of the ultraviolet effective central charge  $c(0)$ . The calculation is just as described in refs. [8, 9], and the desired result  $c(0) = -22/5$  is indeed recovered.

For  $(\Phi(h), \Phi(h'))$ , calculations for the BTCSA are more involved, since two irreducible Virasoro representations appear in the decomposition (3.2) of  $\mathcal{H}_{(\Phi, \Phi)}$ . Work on this is still in progress, but in the meantime we have considered the one case where a simple prediction can be made against which to test conjectures for the BTBA, namely  $h = h' = 0$ . With the boundary fields set to zero, the regular part of  $c(r)$  should exceptionally expand in powers of  $r^{12/5}$ , rather than  $r^{6/5}$ , just as seen for the  $(\mathbb{1}, \Phi(0))$  boundary condition in (5.14). For this case we found unambiguously in favour of a BTBA of the modified type (5.7)–(5.9), with  $\lambda_{\alpha\beta}(\theta) = K_{-0.5}(\theta)K_{-0.5}(-\theta)$ . The fit of  $c(r)$  to the two irregular terms plus a series in  $r^{6/5}$  for this proposal yields

$$\begin{aligned}
c(r)|_{b=b'=-0.5} &= 0.4 - \frac{12(\sqrt{3}-1)(\sqrt{2}-1)}{\pi} r - \frac{2\sqrt{3}}{\pi} r^2 \\
&\quad - 3.89 \times 10^{-12} r^{\frac{6}{5}} + 1.79288 r^{\frac{12}{5}} \\
&\quad - 4.48 \times 10^{-9} r^{\frac{18}{5}} - 0.414179 r^{\frac{24}{5}} - 9.54 \times 10^{-7} r^6 + \dots \quad (7.1)
\end{aligned}$$

As in the earlier fit (5.14), the numerical data is consistent with the coefficients of all odd powers of  $r^{6/5}$  being zero, and this supports the idea that the  $(\Phi(0), \Phi(0))$  ground state is indeed described by the modified BTBA system (5.7)–(5.9). However this conclusion must remain preliminary while a comparison with BTCSA data is lacking, and more work will be needed before we can make any definitive statements about the situation for other values of  $h$  and  $h'$ .

## 8 Conclusions

We hope to have shown that the combination of boundary truncated conformal space and boundary thermodynamic Bethe ansatz techniques allows a detailed analysis to be made of integrable boundary models. Even for a theory as simple as the scaling Lee-Yang model, a rich structure has been revealed. Our results support the contention that the integrable boundary conditions of the model are  $\mathbb{1}$ , with reflection factor  $R_{(1)}(\theta)$ , and the one-parameter family  $\Phi(h)$ , with reflection factors  $R_b(\theta)$ . It is worth pointing out that these latter are a particular subset of the reflection factors

given by Ghoshal in [23] for the lowest breather in the sine-Gordon model, considered at the Lee-Yang point. It is natural to suppose that a boundary variant of quantum group reduction is at work here, and it would be interesting to explore this aspect further. Perhaps even more natural would be to make a link with a reduction of the boundary Bullough-Dodd model, since in that case the classically integrable boundary conditions already lie in a couple of one-parameter families [24].

From BTCSA and BTBA results, and also from a simple consideration of their ultraviolet limits, it is clear that the  $\mathbb{1}$  boundary condition is not the same as the  $\Phi(h)$  boundary condition for any finite value of  $h$ . Nevertheless, we note that  $R_{(1)} = R_{b=0}$ . Thus the infrared data provided by an S-matrix and reflection factor alone is not enough to characterise a boundary condition completely. It is still possible that there is a special relationship between the  $\mathbb{1}$  and  $\Phi(h(b=0))$  boundary conditions, but further numerical work will be required before we can make any definite claims one way or the other.

Finally we would like to reiterate that the boundary scaling Lee-Yang model was studied in this paper just as a first example. The methods that we have used should be applicable in many other situations, and we intend to report on such matters in due course.

**Acknowledgements** — PED thanks Ed Corrigan, and GMTW thanks M. Blencowe, M. Ortiz and I. Runkel for conversations, and A. Honecker for pointing out reference [17]. We would also like to thank Jean-Bernard Zuber for helpful comments. The work was supported in part by a TMR grant of the European Commission, contract reference ERBFMRXCT960012, in part by a NATO grant, number CRG950751, and in part by an EPSRC grant GR/K30667. PED and GMTW thank the EPSRC for Advanced Fellowships, AJP thanks the EPSRC for a Research Studentship, and RT thanks the Mathematics Department of Durham University for a postdoctoral fellowship and SPhT Saclay for hospitality.

**Note** — for some recent work exploring related issues from a slightly different angle, see ref. [25].

## References

- [1] S. Ghoshal and A.B. Zamolodchikov, ‘Boundary  $S$  matrix and boundary state in two-dimensional integrable quantum field theory’, *Int. J. Mod. Phys.* **A9** (1994) 3841, [hep-th/9306002](#).
- [2] I.V. Cherednik, ‘Factorizing particles on a half-line and root systems’, *Teor. Math. Phys.* **61** (1984) 977.

- [3] A. Fring and R. Köberle, ‘Factorized scattering in the presence of reflecting boundaries’, Nucl. Phys. **B421** (1994) 159, [hep-th/9304141](#).
- [4] V.P. Yurov and A.I.B. Zamolodchikov, ‘Truncated conformal space approach to the scaling Lee-Yang model’, Int. J. Mod. Phys. **A5** (1990) 3221.
- [5] A.I.B. Zamolodchikov, ‘Thermodynamic Bethe Ansatz in Relativistic Models. Scaling 3-state Potts and Lee-Yang Models’, Nucl. Phys. **B342** (1990) 695.
- [6] A.B. Zamolodchikov, talk at the 1994 Los Angeles conference ‘Recent progress in statistical mechanics and quantum field theory’ (unpublished).
- [7] A. LeClair, G. Mussardo, H. Saleur and S. Skorik, ‘Boundary energy and boundary states in integrable quantum field theories’, Nucl. Phys. **B453** (1995) 581, [hep-th/9503227](#).
- [8] V.V. Bazhanov, S.L. Lukyanov and A.B. Zamolodchikov, ‘Integrable quantum field theories in finite volume: excited state energies’, Nucl. Phys. **B489** (1997) 487, [hep-th/9607099](#).
- [9] P. Dorey and R. Tateo, ‘Excited states by analytic continuation of TBA equations’, Nucl. Phys. **B482** (1996) 639, [hep-th/9607167](#).
- [10] P. Dorey, A. Pocklington, I. Runkel, R. Tateo and G. Watts, in preparation.
- [11] J.L. Cardy, ‘Conformal invariance and the Yang–Lee edge singularity in two dimensions’, Phys. Rev. Lett. **54** (1985) 1354.
- [12] J.L. Cardy, ‘Boundary conditions, fusion rules and the Verlinde formula’, Nucl. Phys. **B324** (1989) 581.
- [13] J.L. Cardy and D.C. Lewellen, ‘Bulk and boundary operators in conformal field theory’, Phys. Lett. **B259** (1991) 274;  
D.C. Lewellen, ‘Sewing constraints for conformal field theories on surfaces with boundaries’, Nucl. Phys. **B372** (1991) 654.
- [14] J.L. Cardy and G. Mussardo, ‘ $S$  matrix of the Yang–Lee edge singularity in two-dimensions’, Phys. Lett. **B225** (1989) 275.
- [15] A.I.B. Zamolodchikov, ‘Mass scale in sine-Gordon model and its reductions’, Int. J. Mod. Phys. **A10** (1995) 1125.
- [16] R. Sasaki, ‘Reflection bootstrap relations for Toda field theory’, Plenary talk at the International Conference on Interface between Physics and Mathematics IPM93, Hangzhou, China; YITP/U-93-33, [hep-th/9311027](#).
- [17] U. Bilstein and B. Wehefritz, ‘Spectra of non-hermitian quantum-spin chains describing boundary induced phase transitions’, J. Phys. **A30** (1997) 4925, [cond-mat/9611163](#).



- [18] M. Lässig, G. Mussardo and J.L. Cardy, ‘The scaling region of the tricritical Ising model in two dimensions’, Nucl. Phys. **B348** (1991) 591.
- [19] I. Affleck and A.W.W. Ludwig, ‘Universal noninteger “Ground-State Degeneracy” in critical quantum systems’, Phys. Rev. Lett. **67** (1991) 161.
- [20] A.I.B. Zamolodchikov, ‘On the thermodynamic Bethe ansatz equations for reflectionless ADE scattering theories’, Phys. Lett. **B253** (1991) 391.
- [21] P. Dorey and R. Tateo, ‘Excited states in some simple perturbed conformal field theories’, Nucl. Phys. **B515** (1998) 575, [hep-th/9706140](#).
- [22] H.G. Kausch, G. Takács and G.M.T. Watts, ‘On the relation between  $\Phi_{(1,2)}$  and  $\Phi_{(1,5)}$  perturbed minimal models and unitarity’, Nucl. Phys. **B489** (1997) 557, [hep-th/9605104](#).
- [23] S. Ghoshal, ‘Boundary state boundary S-matrix of the sine-Gordon model’, Int. J. Mod. Phys. **A9** (1994) 4801, [hep-th/9310188](#).
- [24] P. Bowcock, E. Corrigan, P.E. Dorey and R.H. Rietdijk, ‘Classically integrable boundary conditions for affine Toda field theories’, Nucl. Phys. **B445** (1995) 469, [hep-th/9501098](#).
- [25] F. Lesage, H. Saleur and P. Simonetti, ‘Boundary flows in minimal models’, USC preprint USC-98-003, [hep-th/9802061](#).